

Inelastic electron scattering and the structure of shell-model nuclei: The ^{40}Ca case

P. Federman

CIEA del IPN, Departamento de Física, Apartado Postal 14-740, México 14, D. F.

T. W. Donnelly

Institute of Theoretical Physics, Department of Physics, Stanford University, Stanford, California 94305
(Received 21 August 1973; revised manuscript received 18 March 1974)

Inelastic electron scattering is shown to be a very powerful tool to study the structure of shell-model nuclei, since the form factors are very sensitive to small admixtures of different orbitals. For instance in our ^{40}Ca case admixtures of only 1% $1p_{3/2}$ orbital in the pure $f_{7/2}$ orbital produce strong changes in the form factors. Thus, inelastic electron scattering will shed light on the question of "deformed states" in ^{40}Ca . Also it is pointed out that "effective" multipole matrix elements can be extracted. In turn, those matrix elements can be used for structure analysis of shell-model nuclei by giving information on which admixtures should be included to reproduce them.

[NUCLEAR STRUCTURE ^{40}Ca ; calculated form factors for inelastic electron scattering.]

I. INTRODUCTION

The advantages of electron scattering as a tool to study nuclear structure have been recognized and pointed out in the past.^{1,2} These advantages stem from the fact that the incident electron interacts with the nucleus via the well known and relatively weak electromagnetic interaction.

However, until now the use of this tool was hampered by the poor energy resolutions attained with available electron accelerators. Thus, data corresponding to groups of levels rather than single levels were usually obtained.

This situation is now about to be changed with the completion of new electron scattering facilities. Their resolution will allow the study of single levels, thus making possible a detailed comparison with the predictions of different nuclear structure models.

In this work we are concerned with what one can learn from electron scattering about the structure of nuclei well described by the shell model. We shall see that the form factors can be very sensitive to different active shell-model orbitals, to the point that one can sometimes detect 1% admixtures in them. As an example we use the low-lying $J^\pi = 0^+$ and 2^+ levels of ^{40}Ca . This case is of particular interest since there are several different descriptions of the structure of ^{40}Ca .³⁻⁶

The electron scattering form factors are matrix elements of one-body operators. They can therefore be reduced to functions of single-particle matrix elements using standard shell-model tech-

niques. The number of different single-particle matrix elements and their quantum numbers depend on the orbitals included in the shell-model calculation.

There are two main approaches to describe the structure of nuclei within the framework of the shell model. One of them relies on a certain form for the nuclear residual interaction, the philosophy being that one should include as many configurations as necessary for this "phenomenological" potential to describe the nuclear states appropriately. The second approach (a la Talmi) is the effective interactions method.⁷ In this approach one reduces as much as possible the number of configurations considered, the effect of the others being included in the "effective" two-body matrix elements. The "effective" matrix elements are empirically determined by fitting known energy levels. One could do something similar for electron scattering, and in this way obtain "effective" single-nucleon multipole matrix elements. But since the electromagnetic interaction is well known, the single-particle matrix elements can be calculated quite accurately and used to obtain the form factors for individual levels.

A detailed comparison with experimental data will then furnish a strong test of the validity of the wave functions used. In this way information on the structure of the wave functions can be obtained by seeing which configurations have to be included in order to fit the experimental form factors.

The calculation carried out here for ^{40}Ca is in this respect of particular interest, since there

are several different descriptions³⁻⁶ for the structure of ⁴⁰Ca. Some are based on the inclusion of deformed rotational bands built on up to 8p-8h (8 particle-8 hole) intrinsic states. The interesting point here is that if the single-particle orbitals are deformed in this region the ⁴⁴Ti spectrum should show a rotational band built on its g.s. (ground state), in analogy to ²⁰Ne in the (2s, 1d) shell. Since this is not the case,⁸ there would seem to exist an inconsistency with the existence of deformed states in ⁴⁰Ca.

Inelastic electron scattering on ⁴⁰Ca may shed some light on this question, since as discussed below the calculated form factors turn out to be very sensitive to the amount of 2p_{3/2} admixtures.

II. DESCRIPTION OF THE CALCULATIONS

A. ⁴⁰Ca wave functions

We have calculated the form factors for all the low-lying $T=0$, 0^+ , and 2^+ states in ⁴⁰Ca. The wave functions were taken from a shell-model description in which configurations up to 4p-4h were included. The particles are in the 1f_{7/2} orbit and the holes in the 1d_{3/2} orbit. All possible intermediate quantum numbers of the configurations $[d_{3/2}^{-n}(v_1 J_1 T_1) f_{7/2}^n(v_2 J_2 T_2)]^{JT}$ ($n=0, 2, 4$) are considered. The wave functions obtained reproduce quite well the energies of all the known 0^+ and 2^+ levels in ⁴⁰Ca, as well as the $E2$ electromagnetic transition rates among them.⁵

In this simple shell-model description of ⁴⁰Ca, the wave function of the i th 0^+ level is given by:

$$\begin{aligned} \psi_i(J^\pi = 0^+, T=0) = & \alpha_i \psi[d_{3/2}^8 0, 0] + \sum_{J_1 T_1} \beta_i (J_1 T_1) \psi[d_{3/2}^6 (J_1 T_1) f_{7/2}^2 (J_1 T_1) 0, 0] \\ & + \sum_{v_0 v'_0 J_0 T_0} \gamma_i (v_0 v'_0 J_0 T_0) \psi[d_{3/2}^4 (v_0 J_0 T_0) f_{7/2}^4 (v'_0 J_0 T_0) 0, 0], \end{aligned} \quad (1)$$

while for the 2^+ states there is no 0p-0h contribution:

$$\begin{aligned} \psi_i(J^\pi = 2^+, T=0) = & \sum_{J_1 J_2 T_1} b_i (J_1 J_2 T_1) \psi[d_{3/2}^6 (J_1 T_1) f_{7/2}^2 (J_2 T_1) 2, 0] \\ & + \sum_{v_1 v_2 J_1 J_2 T_1} c_i (v_1 v_2 J_1 J_2 T_1) \psi[d_{3/2}^4 (v_1 J_1 T_1) f_{7/2}^4 (v_2 J_2 T_1) 2, 0]. \end{aligned} \quad (2)$$

The v 's distinguish among states with the same angular momentum and isospin.

B. Inelastic electron scattering form factors

The inelastic electron scattering form factor from the g.s. to an excited state i , J ($T=0$ always here) is given by⁹:

$$F^2(q) = F_L^2(q) \left(\frac{1}{2} + \tan^2 \frac{1}{2} \theta\right)^{-1} + F_T(q), \quad (3)$$

where the longitudinal term F_L is a function of

$$\langle i, J \| \hat{M}_J^{\text{Coul}}(q) \| \text{g.s.} \rangle$$

only, and $\hat{M}_J^{\text{Coul}}(q)$ is the Coulomb multipole operator.

For the states considered here there is no contribution from the transverse form factor F_T . This follows since there can be no contribution from diagonal single-particle matrix elements because of parity and time reversal invariance.²

Using our shell-model wave functions (1, 2) and standard techniques, the form factors can be reduced to functions of only the single-particle matrix elements. The number of single-particle matrix elements appearing in the expressions for the

form factors depends on the shell-model configurations included in the structure calculation. In our case only two such matrix elements appear for each J . Because the particles are restricted to the 1f_{7/2} and 1d_{3/2} orbits, only

$$\begin{aligned} \langle d_{3/2} \| \hat{M}_J^{\text{Coul}}(q) \| d_{3/2} \rangle, \\ \langle f_{7/2} \| \hat{M}_J^{\text{Coul}}(q) \| f_{7/2} \rangle \end{aligned} \quad (4)$$

TABLE I. Calculated values of $D_i(J)$ and $F_i(J)$ as given by expressions (5) to (8) in the text.

Level	$D_i(J)$	$F_i(J)$
0 ₁	3.603	0.281
0 ₂	0.427	-0.290
0 ₃	-0.451	0.240
0 ₄	0.093	-0.054
0 ₅	0.123	-0.096
2 ₁	0.176	0.097
2 ₂	0.101	0.182
2 ₃	-0.331	0.206
2 ₄	0.126	0.205
2 ₅	0.075	-0.115
2 ₆	-0.036	0.070
2 ₇	-0.021	-0.142

occur in (3). The nondiagonal matrix element vanishes because $1d_{3/2}$ and $1f_{7/2}$ have opposite parity. Thus, we can write

$$\langle i, J \| \hat{M}_J^{\text{Coul}}(q) \| \text{g.s.} \rangle = D_i(J) \langle d_{3/2} \| \hat{M}_J^{\text{Coul}} \| d_{3/2} \rangle + F_i(J) \langle f_{7/2} \| \hat{M}_J^{\text{Coul}} \| f_{7/2} \rangle.$$

For $J = 2$ we obtain:

$$\begin{aligned} D_i(2) = & 6 \sum_{J_0, T_0, J} b_i(JJ_0T_0) \beta_{\text{g.s.}}(J_0T_0) (2J_1 + 1)^{1/2} \\ & \times (-1)^{J_1} \sum_{J'T'} [d_{3/2}^6 J_1 T_0 \{ | d_{3/2}^5(J'T') d_{3/2} J_1 T_0 \} \\ & \times [d_{3/2}^5(J'T') d_{3/2} J_0 T_0 \{ | d_{3/2}^6 J_0 T_0 \}] (-1)^{J'+3/2} \begin{pmatrix} \frac{3}{2} & J_1 & J' \\ J_0 & \frac{3}{2} & 2 \end{pmatrix} \\ & + 4 \sum_{v_0 v'_0 v_1 J_0 T_0 J_1} c_i(v_1 v'_0 J_1 J_0 T_0) \gamma_{\text{g.s.}}(v_0 v'_0 J_0 T_0) (2J_1 + 1)^{1/2} \\ & \times (-1)^{J_1} \sum_{J'T'} [d_{3/2}^4 v_1 J_1 T_0 \{ | d_{3/2}^3(J'T') d_{3/2} J_1 T_0 \} \\ & \times [d_{3/2}^3(J'T') d_{3/2} J_0 T_0 \{ | d_{3/2}^4 v_0 J_0 T_0 \}] (-1)^{J'+3/2} \begin{pmatrix} \frac{3}{2} & J_1 & J' \\ J_0 & \frac{3}{2} & 2 \end{pmatrix}, \end{aligned} \quad (5)$$

and

$$\begin{aligned} F_i(2) = & 2 \sum_{J_0 T_0 J_2} b_i(J_0 J_2 T_0) \beta_{\text{g.s.}}(J_0 T_0) (-1)^{J_0+1} (2J_2 + 1)^{1/2} \begin{pmatrix} \frac{7}{2} & J_2 & \frac{7}{2} \\ J_0 & \frac{7}{2} & 2 \end{pmatrix} \\ & + 4 \sum_{v_0 v'_0 v_2 J_0 T_0 J_2} c_i(v_0 v_2 J_0 J_2 T_0) \gamma_{\text{g.s.}}(v_0 v'_0 J_0 T_0) (-1)^{J_0} (2J_2 + 1)^{1/2} \\ & \times \sum_{v' J' T'} [f_{7/2}^4 v_2 J_2 T_0 \{ | f_{7/2}^3(v' J' T') f_{7/2} J_2 T_0 \} \\ & \times [f_{7/2}^3(v' J' T') f_{7/2} J_0 T_0 \{ | f_{7/2}^4 v'_0 J_0 T_0 \}] (-1)^{J'+7/2} \begin{pmatrix} \frac{7}{2} & J_2 & J' \\ J_0 & \frac{7}{2} & 2 \end{pmatrix}, \end{aligned} \quad (6)$$

where $(v_0 J_0 T_0)$ and $(v'_0 J_0 T_0)$ are intermediate quantum numbers of the ground state wave function as given by (1) and $(v_1 J_1 T_1)$, $(v_2 J_2 T_2)$ the ones of the excited 2^+ states as given by (2).

For the $J = 0$ case, the formulas are simpler:

$$\begin{aligned} D_i(0) = & 4\alpha_i \alpha_{\text{g.s.}} + 3 \sum_{J_0 T_0} \beta_{\text{g.s.}}(J_0 T_0) \beta_i(J_0 T_0) \\ & + 2 \sum_{v_0 v'_0 J_0 T_0} \gamma_{\text{g.s.}}(v_0 v'_0 J_0 T_0) \gamma_i(v_0 v'_0 J_0 T_0), \end{aligned} \quad (7)$$

and

$$\begin{aligned} F_i(0) = & \frac{1}{\sqrt{2}} \sum_{J_0 T_0} \beta_{\text{g.s.}}(J_0 T_0) \beta_i(J_0 T_0) \\ & + \sqrt{2} \sum_{v_0 v'_0 J_0 T_0} \gamma_{\text{g.s.}}(v_0 v'_0 J_0 T_0) \gamma_i(v_0 v'_0 J_0 T_0). \end{aligned} \quad (8)$$

Once the wave functions are given, the functions $D_i(J)$ and $F_i(J)$ can be calculated from expressions (5) to (8), and with them the form factors (3) for each level.

III. RESULTS AND DISCUSSION

As mentioned above, in the present case all form factors can be reduced to functions of only two single-nucleon matrix elements, and the electromagnetic part of those matrix elements can be calculated quite accurately. Formula (4) immediately suggests that one could extract "effective" single-particle matrix elements, the inverted commas meaning that those matrix elements would contain the "unknowns" arising from the nuclear wave function.

Of course this is assuming that the structure

model furnishing the $D_i(J)$ and $F_i(J)$ is the appropriate one. The usefulness of such a method would diminish with increasing number of active single-particle orbits, but much less drastically than in energy levels calculations where two-particle matrix elements are involved.

It would be quite extraordinary if only two parameters could reproduce the inelastic electron scattering form factors for all the levels with the same J , and over the whole range of the momentum transfer q .

The values of the $D_i(J)$ and $F_i(J)$ for the wave functions used here are listed in Table I.

The matrix elements (4) were calculated using harmonic oscillator single-particle wave functions, with oscillator parameter $b = 2.03$ fm.⁹

In order to estimate the influence of $1p_{3/2}$ admixtures, we replaced the $1f_{7/2}$ matrix element in (4) by a linear combination of the $1f_{7/2}$ and $1p_{3/2}$ diagonal matrix elements. The results are quite striking. Writing

$$\alpha |f_{7/2}\rangle + (1 - \alpha^2)^{1/2} |2p_{3/2}\rangle$$

instead of

$$|1f_{7/2}\rangle$$

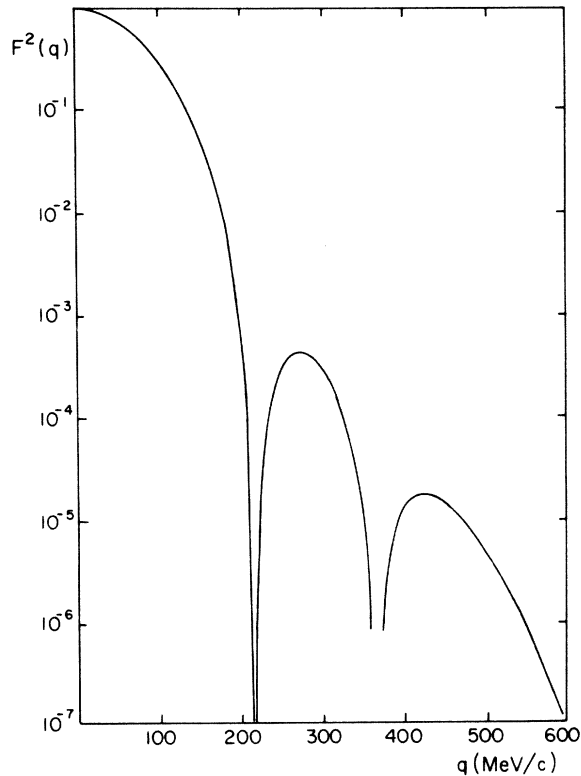


FIG. 1. Elastic form factor for $\alpha = 0$.

and varying α we obtain the form factors shown in Fig. 1 for the elastic form factor ($\alpha = 0$) and in Figs. 2 to 9 for the first two excited $J = 0^+$ and $J = 2^+$ levels of ^{40}Ca .

As can be seen in those figures, in some cases one obtains significant changes with just 1% admixture of $2p_{3/2}$ ($\alpha = \pm 0.1$). For high momentum transfers ($q > 300$ MeV) such a small admixture produces in some cases a change of one order of magnitude for the form factor (see e.g. Fig. 3 for $q \sim 500$ MeV). An admixture of 16% ($\alpha = \pm 0.4$) produces important modifications in practically all cases considered here. Also, the positions of maxima change. This strong effect on the form factors for $\alpha \neq 0$ can be understood when one realizes that the $1f_{7/2}$ and $2p_{3/2}$ single-particle form factors are out of phase. Thus, interference occurs and coherence effects are important.

A few words of caution. Since for transverse form factors²

$$\langle 1f_{7/2} \| T_J^E \| 2p_{3/2} \rangle = -\langle 2p_{3/2} \| T_J^E \| 1f_{7/2} \rangle,$$

there is no contribution to the transverse form factors even if $\alpha \neq 0$, when we use the present method of estimating the influence of the $2p_{3/2}$ or-

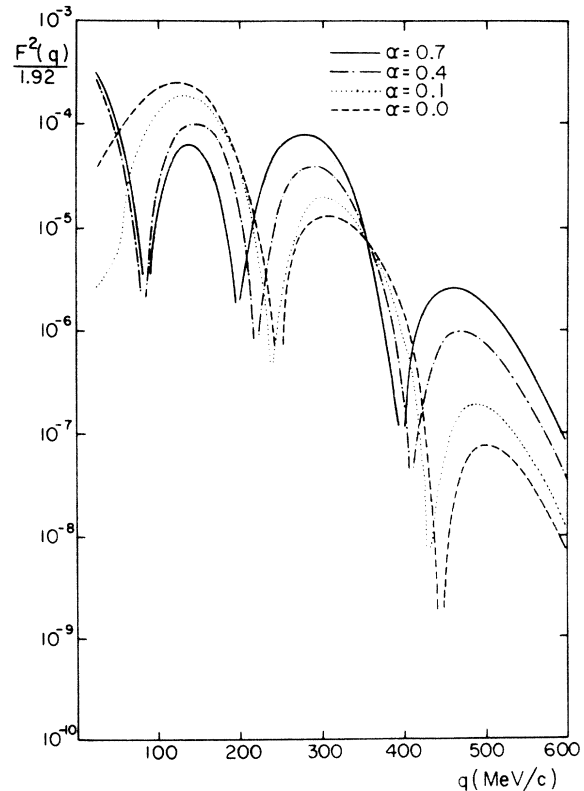


FIG. 2. Inelastic form factors for the first excited 0^+ level in ^{40}Ca , for $\alpha = 0.0, 0.1, 0.4,$ and 0.7 .

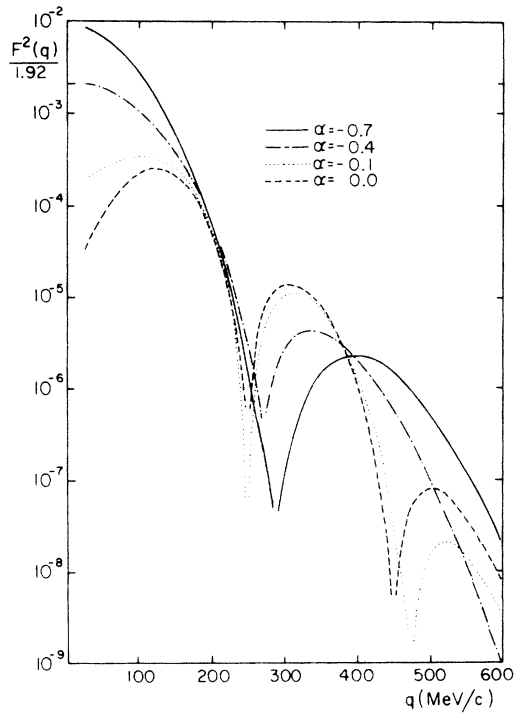


FIG. 3. Inelastic form factors for the first excited 0^+ level in ^{40}Ca , for $\alpha = 0.0, -0.1, -0.4,$ and -0.7 .

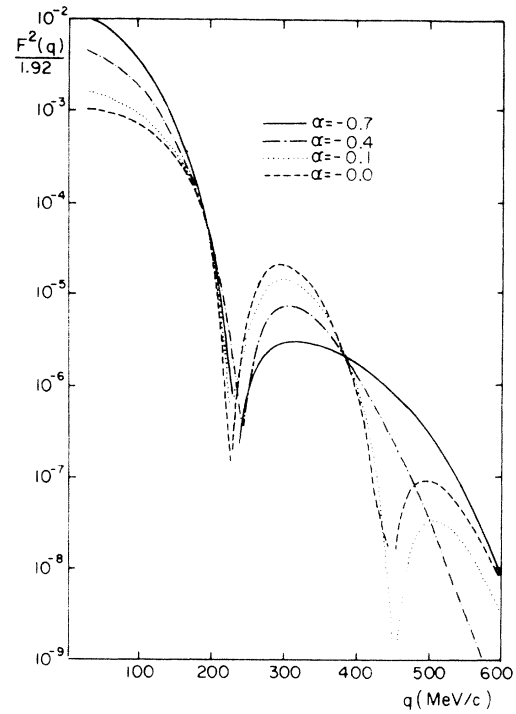


FIG. 5. Inelastic form factors for the second excited 0^+ level in ^{40}Ca , for $\alpha = 0.0, -0.1, -0.4,$ and -0.7 .

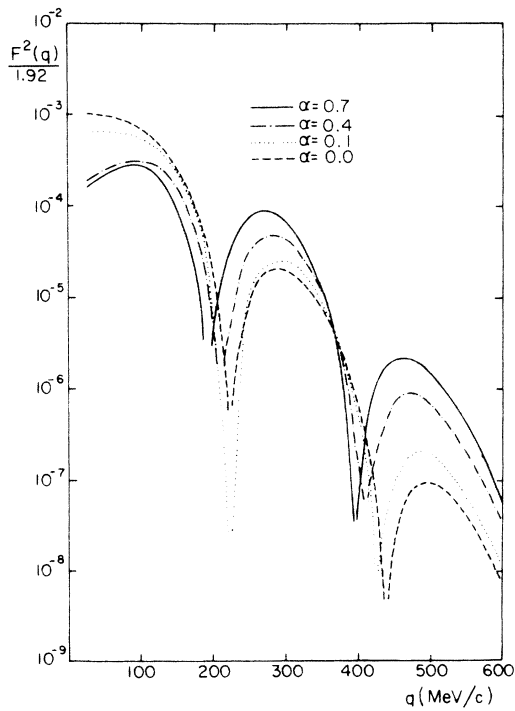


FIG. 4. Inelastic form factors for the second excited 0^+ level in ^{40}Ca , for $\alpha = 0.0, 0.1, 0.4,$ and 0.7 .

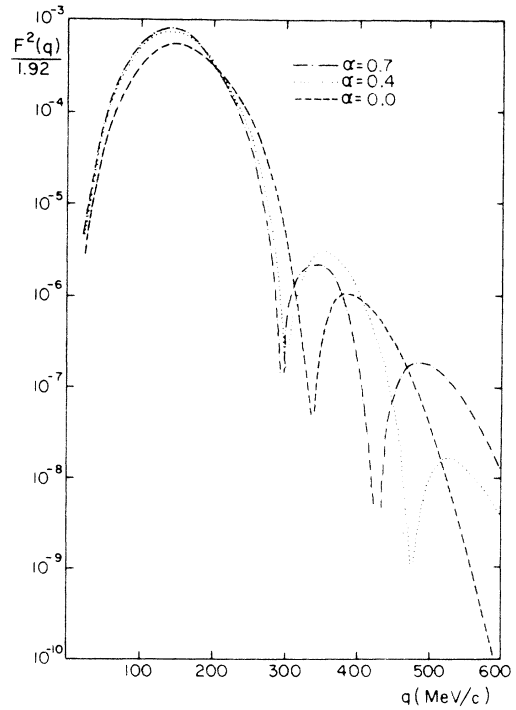


FIG. 6. Inelastic form factors for the first excited 2^+ level in ^{40}Ca , for $\alpha = 0.0, 0.4,$ and 0.7 .

bital. A more realistic consideration of $2p_{3/2}$ admixtures would give some contribution which could tend to smear out the differences in the form factors. But such a contribution could be easily detected at large angles, when the factor $1 + \tan^2 \frac{1}{2} \theta$ makes the contribution of the transverse form factor dominant [see Eq. (3)].

For reasons of space, we do not give here either the form factors for the rest of the excited 0^+ and 2^+ states or the tables of the form factors as a function of q and α , but they are available upon request.

The form factor for elastic scattering is given in Fig. 1 for $\alpha=0$. It practically does not change with α , and the maxima and minima agree well with experiment.¹⁰

In the figures the scale is marked $F^2(q)/1.92$, since $\frac{1}{2} + \tan^2 \frac{1}{2} \theta$ in (3) with $\theta = 100^\circ$ equals 1.92.

Finally, to check the sensitivity of these results to the radial form of the single-particle wave functions, the calculations were repeated using Woods-Saxon wave functions. A potential with radius 4.5 fm, diffuseness 0.65 fm, central well depth 44.2 MeV, and spin-orbit well depth 4.8 MeV was used. This yielded single-particle wave functions with the appropriate separation energies⁹ for the states considered here. The form factors which resulted

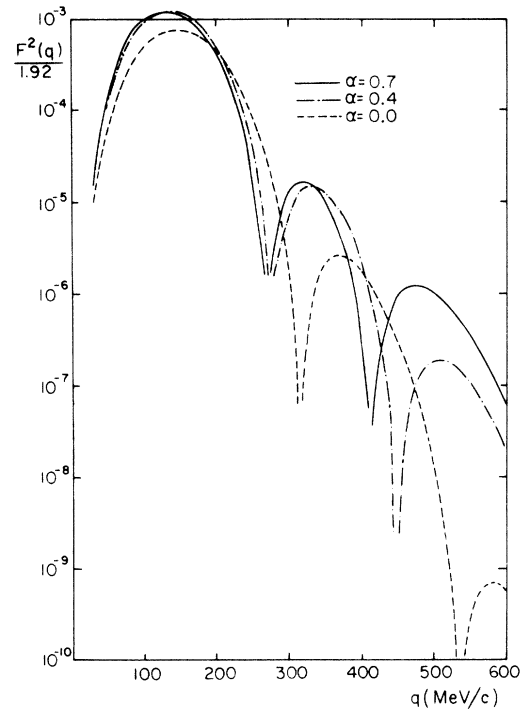


FIG. 8. Inelastic form factors for the second excited 2^+ level in ^{40}Ca , for $\alpha = 0.0, 0.4,$ and 0.7 .

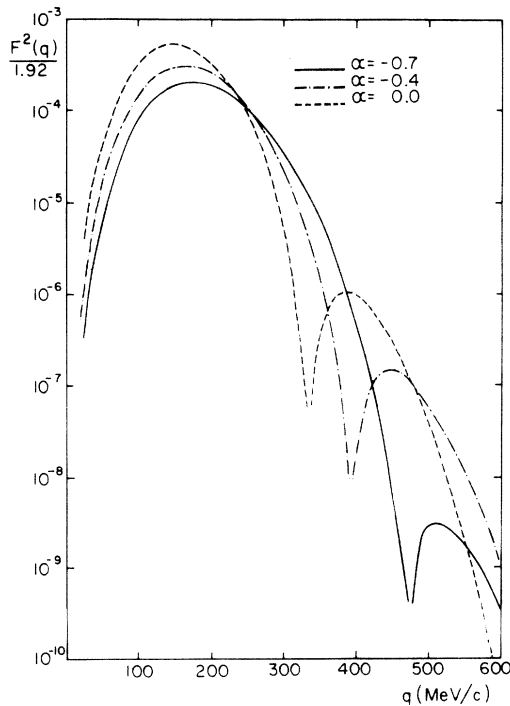


FIG. 7. Inelastic form factors for the first excited 2^+ level in ^{40}Ca , for $\alpha = 0.0, -0.4,$ and -0.7 .

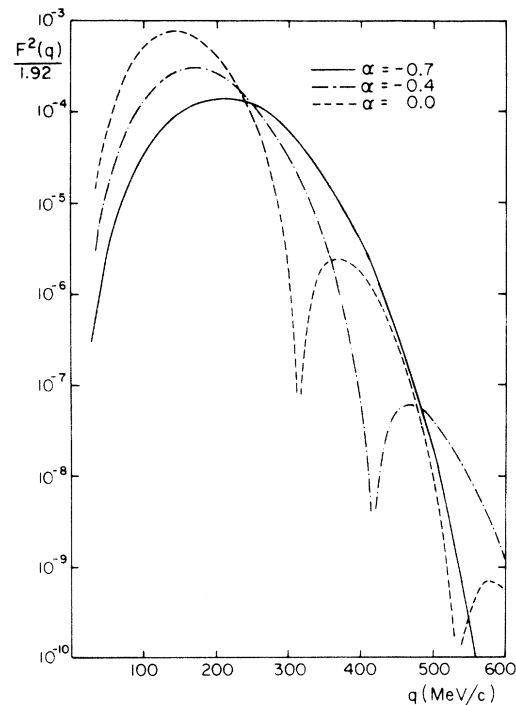


FIG. 9. Inelastic form factors for the second excited 2^+ level in ^{40}Ca , for $\alpha = 0.0, -0.4,$ and -0.7 .

when these radial wave functions replaced the harmonic oscillator wave functions (but with the configuration admixtures exactly the same) were essentially the same as those presented in the figures. Within the scope of the simple model used in the present work it is not necessary to use Woods-Saxon wave functions, but it is sufficient to calculate form factors with harmonic oscillators whose simple analytic form can be exploited to greatly simplify the computational problems involved. (A similar conclusion was reached in a different but related context.¹¹) Of course if very accurate experimental data become available and if a full-scale attack is launched on the problem of configuration mixing, then it may be necessary to refine the single-particle wave functions and worry about the 10–20% differences found at medium to high momentum transfers in the present work.

IV. CONCLUSIONS

Experiment will furnish information that can and should be used in two different ways for nuclear structure analysis.

We have seen that inelastic electron scattering is a very powerful tool for studying the structure of shell-model nuclei since the form factors are *very* sensitive to small configuration admixtures, at least when the single-particle form factors are out of phase. Thus experiment can furnish a strong test for their wave functions and the model that produced them.

In the particular case treated in this work, namely ⁴⁰Ca, our treatment of $2p_{3/2}$ admixtures is equivalent to replacing the spherical shell-model orbital $1f_{7/2}$ by a deformed Nilsson-like orbital. Thus, the form factors for inelastic electron scattering will provide a strong test of the assumption of the exist-

tence of deformed states in ⁴⁰Ca. Since in the case of a deformed state α must be quite large, the form factors will be *very* different, and their measurement should help decide on the question about the existence of deformed states in the Ca region.

On the other hand, the wave functions used here were obtained by the “effective interactions” method. That means that using the pure $1f_{7/2}$ and $1d_{3/2}$ harmonic oscillator orbitals to calculate the matrix elements (4) could be an oversimplification. It may well be that the “effective” $1f_{7/2}$ and $1d_{3/2}$ orbitals are quite different from their harmonic oscillator versions. One could then see if for electron scattering there are “effective” multipole matrix elements (4) that reproduce the experimental form factors with the “effective” wave functions. Notice that in our ⁴⁰Ca case only four such “effective” single-particle matrix elements would have to reproduce *all* 0^+ and 2^+ form factors for *all* q . Namely, it is quite a stringent test, and if four such matrix elements exist they must be meaningful. Having found these “effective” matrix elements, we can then see which admixtures of neglected orbitals are needed to reproduce them. Since the electromagnetic interaction is well known this would provide information on configuration admixtures. The equivalent could not be done with nuclear interaction “effective” matrix elements because the nuclear interaction is *not* well known. Again, the nature of the interaction is the advantage of electron scattering.

ACKNOWLEDGMENTS

One of us (P. F.) would like to thank Professor S. Hanna and Professor D. Walecka for the warm hospitality extended to him at Stanford during the summer of 1972, when this work was started.

¹R. Hofstadter, *Annu. Rev. Nucl. Sci.* **7**, 231 (1957); *Rev. Mod. Phys.* **28**, 214 (1956).

²T. de Forest, Jr., and J. D. Walecka, *Adv. Phys.* **15**, 1 (1966).

³W. J. Gerace and A. M. Green, *Nucl. Phys.* **A93**, 110 (1967); **A123**, 241 (1969).

⁴L. Zamick, *Ann. Phys. (N. Y.)* **47**, 182 (1968).

⁵P. Federman, *Nucl. Phys.* **A124**, 363 (1969); P. Federman and S. Pittel, *Phys. Rev.* **186**, 1106 (1969); *Nucl. Phys.* **A139**, 108 (1969).

⁶L. B. Hubbard, J. B. McGrory, and H. P. Jolly, *Phys. Rev. C* **6**, 532 (1972).

⁷I. Talmi, *Rev. Mod. Phys.* **34**, 704 (1962).

⁸W. R. Dixon and R. S. Storey, *Nucl. Phys.* **A202**, 579 (1973).

⁹T. W. Donnelly and G. E. Walker, *Ann. Phys. (N. Y.)* **60**, 209 (1970).

¹⁰M. Croissiaux *et al.*, *Phys. Rev.* **137**, B865 (1965).

¹¹T. W. Donnelly and J. D. Walecka, *Nucl. Phys.* **A201**, 81 (1973).